

Dalton Transactions

Accepted Manuscript



This is an *Accepted Manuscript*, which has been through the Royal Society of Chemistry peer review process and has been accepted for publication.

Accepted Manuscripts are published online shortly after acceptance, before technical editing, formatting and proof reading. Using this free service, authors can make their results available to the community, in citable form, before we publish the edited article. We will replace this *Accepted Manuscript* with the edited and formatted *Advance Article* as soon as it is available.

You can find more information about *Accepted Manuscripts* in the [Information for Authors](#).

Please note that technical editing may introduce minor changes to the text and/or graphics, which may alter content. The journal's standard [Terms & Conditions](#) and the [Ethical guidelines](#) still apply. In no event shall the Royal Society of Chemistry be held responsible for any errors or omissions in this *Accepted Manuscript* or any consequences arising from the use of any information it contains.

Cite this: DOI: 10.1039/c0xx00000x

www.rsc.org/xxxxxx

ARTICLE TYPE

Synthesis, Crystal Structure and Study of Magnetocaloric Effect and Single Molecular Magnetic Behaviour in Discrete Lanthanide Complexes[#]

Amit Adhikary, Javeed Ahmad Sheikh, Soumava Biswas and Sanjit Konar*

Department of Chemistry, IISER Bhopal, Bhopal- 462066, India, Fax: (+91) 7556692392.

Received (in XXX, XXX) Xth XXXXXXXXX 20XX, Accepted Xth XXXXXXXXX 20XX

DOI: 10.1039/b000000x

The synthesis, crystal structure and magnetic properties of four polynuclear lanthanide coordination complexes having molecular formulae, $[\text{Gd}_3\text{L}^1_2(\text{H}_2\text{O})_8(\text{Cl})(\text{Cl})_4 \cdot 10\text{H}_2\text{O}$ (**1**), $[\text{Dy}_3\text{L}^1_2(\text{H}_2\text{O})_9(\text{Cl})_5 \cdot 6\text{H}_2\text{O}$ (**2**), $[\text{Gd}_6\text{L}^2_2(\text{HCO}_2)_4(\mu_3\text{-OH})_4(\text{DMF})_6(\text{H}_2\text{O})_2](\text{Cl})_2 \cdot 4\text{H}_2\text{O}$ (**3**) and $[\text{Dy}_6\text{L}^2_2(\text{HCO}_2)_4(\mu_3\text{-OH})_4(\text{DMF})_6(\text{H}_2\text{O})_2](\text{Cl})_2 \cdot 4\text{H}_2\text{O}$ (**4**) (where $\text{H}_2\text{L}^1 = \text{bis}[(2\text{-pyridyl)methyl]pyridine-2,6\text{-dicarbohydrazide}$ and $\text{H}_4\text{L}^2 = \text{bis}[2\text{-hydroxy-benzylidene]pyridine-2,6\text{-dicarbohydrazide}$) are reported. Structural investigation by x-ray crystallography reveals similar structural features for complexes **1** and **2** and they exhibit butterfly like shape of the molecule. Non-covalent interactions between the molecules create double helical arrangements for both the molecules. Complexes **3** and **4** are iso-structural and the core structures feature four distorted hemi-cubanes connected by vertex sharing. Magnetic studies unveil significant magnetic entropy changes for complexes **1**, **3** and slow relaxation of magnetization for both the dysprosium analogues **2** and **4**.

Introduction

Lanthanide based molecular magnetic materials are a forefront area of research owing to their proposed applications which accounts for their appealing candidature for future devices like molecular magnets,¹ magnetic refrigerants² etc. Choice of lanthanides as magnetic centers are due to their large spins and abundance of two distinct metal ions one of which shows isotropic (Gd^{3+}) and the other anisotropic (Dy^{3+}) magnetic behavior. Till date significant number of magnetic refrigerant materials with gadolinium as a constituent element have been documented in the literature³⁻⁷ because of its highly favoured large spin ground state, quenched orbital momentum and weak super exchange interactions. On the other hand, the intrinsic magnetic anisotropy and the increased number of unpaired f-electrons may be responsible for the high energy barrier for reversal of magnetization in dysprosium and is thereby exhibit SMM behaviour.⁸⁻¹⁰ This interest has led to consistently synthesize new molecules with a finite number of interacting magnetic centers suitable for detailed magnetic study. Polytopic hydrazone based ligands are of wide importance in this context owing to their candidature for the synthesis of polymetallic systems and nanosized supramolecular objects. Although employing polypyridyl ligands, significant contribution has already been documented in the literature,^{1,2,4-7} yet the systematic

approaches for the inclusion of large numbers of metal ions in a small, single molecular entity with interesting functional properties¹¹ is a synthetic challenge and is of current research interest. In this work, we report synthesis of two new flexible and multidentate ligands, namely, bis[(2-pyridyl)methyl]pyridine-2,6-dicarbohydrazide (H_2L^1) and bis[2-hydroxy benzylidene]pyridine-2,6-dicarbohydrazide (H_4L^2) (Fig. 1) and successfully isolated four lanthanide coordination complexes with the ligands having molecular formulae, $[\text{Gd}_3\text{L}^1_2(\text{H}_2\text{O})_8(\text{Cl})(\text{Cl})_4 \cdot 10\text{H}_2\text{O}$ (**1**), $[\text{Dy}_3\text{L}^1_2(\text{H}_2\text{O})_9(\text{Cl})_5 \cdot 6\text{H}_2\text{O}$ (**2**), $[\text{Gd}_6\text{L}^2_2(\text{HCO}_2)_4(\mu_3\text{-OH})_4(\text{DMF})_6(\text{H}_2\text{O})_2](\text{Cl})_2 \cdot 4\text{H}_2\text{O}$ (**3**), and $[\text{Dy}_6\text{L}^2_2(\text{HCO}_2)_4(\mu_3\text{-OH})_4(\text{DMF})_6(\text{H}_2\text{O})_2](\text{Cl})_2 \cdot 4\text{H}_2\text{O}$ (**4**).

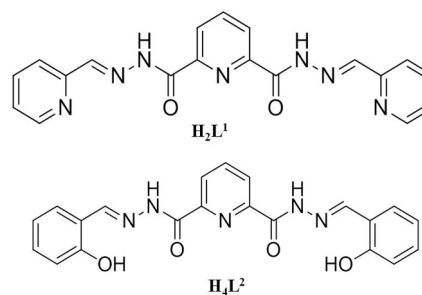


Fig. 1. Schematic drawing of the ligands H_2L^1 (top) and H_4L^2 (bottom).

Structural investigation by X-ray crystallography reveals butterfly like molecular shape for complexes **1** and **2**. They further engender double helical arrangement in solid state *via* non-covalent interactions. Complexes **3** and **4** are isostructural where core structures formed by four hemi-cubanes sharing common vertices. Magnetic studies reveal that complexes **1** and **3** show large cryogenic magnetic entropy changes and single molecular magnetic behaviour for complexes **2** and **4**.

10 Experimental

Materials and methods

X-ray Crystallography. X-ray crystallographic data for complexes **1-4** were collected at 120 K on a Bruker Smart Apex2 CCD diffractometer using graphite monochromated MoK α ($\lambda = 0.71073$) radiation. Data collections were performed using φ and ω scan. The structures were solved using direct methods followed by full matrix least square refinements against F^2 (all data HKLF 4 format) using SHELXTL.¹² Anisotropic refinement was used for all non-hydrogen atoms. Organic hydrogen atoms were placed in appropriate calculated positions. For the solvent accessible voids of complexes **1-3** PLATON-SQUEEZE¹³ procedure were applied. For the complex **1**, only 13 electrons were accounted and this is sufficiently small for any solvent molecule. So extra solvent molecules were not added. For the complex **2**, 28 electrons were recovered and one water molecule was counted as observed from TG analysis. For the complex **3**, 33 electrons were counted and two water molecules were identified. For the complex **1**, high U_{eq} values of C4 atom and related atoms are due to the disorderness of the ring. For the complex **2**, high U_{eq} values of O6w atom is due to disorderness of the free solvent. For the complex **3**, bad ellipsoid of O12/C13 and high U_{eq} values of C3 and C104 atoms are due to the disorderness of the DMF solvent. X-ray crystallographic data in CIF format are available in CCDC 941241-941244 (www.ccdc.cam.ac.uk/data_request/cif). Crystallographic parameters of the complexes **1-4** are given in Table 1.

Materials and Methods. The reagents were used as received from Sigma Aldrich chemical company without further purification. Infrared Spectra were recorded in the solid state (KBr pellets) on a Perkin Elmer FTIR spectrometer in the range of 400-4000 cm^{-1} . Thermo-gravimetric analyses were recorded on Perkin-Elmer TGA 4000 instrument. Elemental analyses were performed on an Elementar vario Microcube elemental analyzer. Variable temperature direct current (dc) and alternating current (ac) magnetic susceptibility data were collected on a quantum design SQUID-VSM magnetometer equipped with a 7 T magnet. The measured values were corrected for the experimentally measured contribution of the sample holder, while the derived susceptibilities were corrected for the diamagnetism of the samples, estimated from Pascal's tables.¹⁴ AC magnetic susceptibilities were performed in 3.5 G field oscillating at 1-780 Hz in the 1.8-10 K temperature range.

Synthesis

The ligands H_2L^1 and H_4L^2 were synthesized following previously reported procedures.¹⁵

[Gd₃L¹₂(H₂O)₈(Cl)](Cl)₄·10H₂O (1**):** H_2L^1 (75 mg, 0.2 mmol) was taken in 10 mL methanol in a round bottom flask and

triethylamine (40 mg, 0.4 mmol) was added drop wise into it while stirring. After that $\text{GdCl}_3 \cdot 6\text{H}_2\text{O}$ (148.4 mg, 0.4 mmol) was added in parts and the solution was stirred further for 3 h and filtered. The filtrate was kept for crystallization at room temperature. After one week, pale yellow coloured single crystals were obtained and separated by filtration. The crystals were washed with diethyl ether and dried in air. Elemental analysis (%): Calcd.(found) for $(\text{C}_{38}\text{H}_{62}\text{Gd}_3\text{O}_{22}\text{N}_{14}\text{Cl}_5)$: C, 26.60(26.92); H, 3.64(3.22); N, 11.43(11.68). Selected IR data (KBr pellet): 3179.4(b), 1672.6(s), 1592.6(w), 1567.4(m), 1534.8(s), 1437.6(w), 1305.8(m), 1236.5(m), 1154.7(s), 999.5(m), 746.3(m) cm^{-1}

[Dy₃L¹₂(H₂O)₉](Cl)₅·6H₂O (2**):** Complex **2** was prepared following the same procedure as for **1** but $\text{DyCl}_3 \cdot 6\text{H}_2\text{O}$ (150.7 mg, 0.4 mmol) was taken as metal salt instead of $\text{GdCl}_3 \cdot 6\text{H}_2\text{O}$. After one week, yellow coloured single crystals were separated by filtration and washed with diethyl ether and dried in air. Elemental analysis: Calcd.(found) for $(\text{C}_{38}\text{H}_{56}\text{Dy}_3\text{O}_{19}\text{N}_{14}\text{Cl}_5)$: C, 27.02(26.17); H, 3.36(3.25); N, 11.69(11.50). Selected IR data (KBr pellet): 3108.4(b), 1701.4(s), 1625.3(w), 1595.2(m), 1475.1(s), 1426.3(m), 1328.2(m), 1228.3(m), 1157.3(s), 999.8(m), 770.5(m) cm^{-1}

[Gd₆L²₂(HCO₂)₄(μ_3 -OH)₄(DMF)₆(H₂O)₂](Cl)₂·4H₂O (3**):** H_4L^2 (81 mg, 0.2 mmol) was taken in 15 mL of 5:1 MeOH : DMF mixture in a round bottom flask and triethylamine (80 mg, 0.8 mmol) was added drop wise into it. After that $\text{GdCl}_3 \cdot 6\text{H}_2\text{O}$ (148.4 mg, 0.4 mmol) was added in parts to the solution and it was stirred for 1 h. After 1 h, ammonium formate (12.6 mg, 0.2 mmol) was added in parts and stirred for 2 h more. Then the solution was filtered and the filtrate was kept for crystallization at room temperature. After few weeks, pale yellow coloured single crystals were obtained and separated by filtration. The crystals were washed with diethyl ether and dried in air. Elemental analysis: Calcd.(found) for $\text{C}_{64}\text{H}_{88}\text{Cl}_2\text{Gd}_6\text{N}_{16}\text{O}_{32}$: C, 29.48(29.63); H, 3.40(3.60); N, 8.59(8.41). Selected IR data (KBr pellet): 3261.5(b), 1636.1(s), 1546.3(m), 1474.6(m), 1397.3(m), 1033.6(s), 818.2(m), 745.9(m) cm^{-1} .

[Dy₆L²₂(HCO₂)₄(μ_3 -OH)₄(DMF)₆(H₂O)₂](Cl)₂·4H₂O (4**):** Complex **4** was prepared following the same procedure as for **3** but $\text{DyCl}_3 \cdot 6\text{H}_2\text{O}$ (150.7 mg, 0.4 mmol) was taken as metal salt instead of $\text{GdCl}_3 \cdot 6\text{H}_2\text{O}$. After one week, pale yellow coloured single crystals were separated by filtration, washed with diethyl ether and dried in air. Elemental analysis: Calcd.(found) for $\text{C}_{64}\text{H}_{88}\text{Cl}_2\text{Dy}_6\text{N}_{16}\text{O}_{32}$: C, 29.12(29.34); H, 3.36(2.98); N, 8.49(8.75). Selected IR data (KBr pellet): 3340.1(b), 1612.4(s), 1544.8(m), 1474.2(s), 1398.9(s), 1036.1(s), 903.1(m), 765.2(m) cm^{-1} .

RESULTS AND DISCUSSIONS:

Synthetic aspects. Reaction of hydrazone based ligand, H_2L^1 and Ln^{III} ($\text{Ln} = \text{Gd}, \text{Dy}$) chloride salts in methanol in presence of triethylamine as a base resulted in the trinuclear complexes **1** and **2** under ambient conditions. Upon changing the terminal pockets of the tri-topic ligand to H_4L^2 under similar conditions but in presence of a co-ligand (formate) hexanuclear complexes **3** and **4** were obtained. However, addition of co-ligand in the synthesis of **1** and **2**, resulted no change in final product. We also have carried out similar reactions from where complexes **3** and **4** were

isolated, but without adding co-ligand formate. However, the crystals obtained were not suitable for diffraction and we were unable to characterize the final product. Thermogravimetric analysis (TGA) of complex **1** shows that weight loss of ~ 19.1 % (calc. 18.9 %) in the temperature range of 40-170°C corresponding to the weight loss of ten solvent water and eight coordinated water molecules (Fig. S1). For the complex **2**, for the weight loss of ~ 16.0 % (calc. 16.1 %) in the temperature range of 40-170°C corresponds to the weight loss of six solvent water and nine coordinated water molecules (Fig. S2). Similarly weight loss of ~ 20.8 % (calc. 20.9 %) for complex **3** and weight loss of ~ 20.0 % (calc. 20.7%) of complex **4** in the temperature range of 35-180°C corresponds to four solvent water, two coordinated water and six coordinated DMF molecules (Fig. S3, S4).

Structural Description for 1

Structural investigation by single crystal X-ray crystallography shows that complex **1** crystallizes in *C2/c* space group. It comprises of two ligands $[L^1]^{2-}$, three Gd^{3+} , one coordinated Cl^- anion, eight coordinated water molecules, four non-coordinated Cl^- anions and ten non-coordinated water molecules (Fig. 2) in the crystal lattice. Two ligands bind three Gd^{3+} ions in a twisted fashion at an angle of 71.39° resulting in a butterfly like shape (Fig. 2). All the Gd^{3+} centers are nine coordinated showing tri-capped trigonal prismatic geometry with N_2O_6Cl (Gd1) and N_4O_5 (Gd2 and Gd2') coordination environments (Fig. S5). Adjacent Gd^{3+} ions are connected by two μ_2 -O bridges from hydrazone oxygen of two ligands with bridging angles in the range of 117 - 117.8° . Distances between neighboring Gd^{3+} ions are 4.197 Å. Gd - O bond distances are lying in the range of $2.390(5)$ - 2.541 Å and Gd-N bond distances are lying in the range of $2.570(4)$ Å to $2.656(5)$ Å. Interestingly, each entity of complex is regularly stacked one on top of the other maintaining proper registry to form various intra-molecular (Fig. S6) and intermolecular (Fig. S7) hydrogen bonded (Table S1) double helical arrangement along the crystallographic *a* axis (Fig. 4, left).

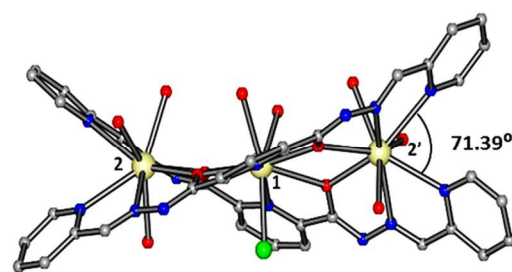


Fig. 2. Ball & stick model showing molecular structure of complex **1** in the crystal. Hydrogen atoms and solvents are omitted for clarity. Colour code: pale yellow, gadolinium; red, oxygen; blue, nitrogen; gray, carbon; green, chlorine.

Structural Description for 2

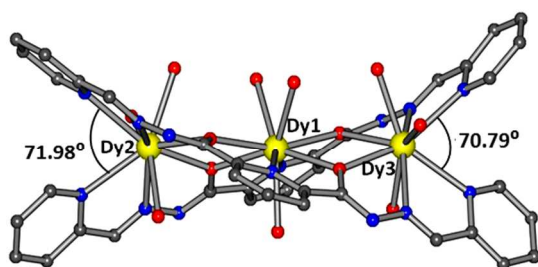
Structure of complex **2** is similar with **1**. However it was crystallized in *P-1* space group. It consists of two ligands $[L^1]^{2-}$, three Dy^{3+} , five non-coordinated Cl^- anions, nine coordinated water molecules and six non-coordinated water molecules (Fig. 2) in the crystal lattice. Here two ligands bind three Dy^{3+} ions in a twisted fashion at an angle of 71.98° in one side and at an angle of 70.79° for other side (Fig. 3). All the Dy^{3+} centers are nine coordinated showing tri-capped trigonal prismatic geometry (Fig. S8) with N_2O_7 (Dy1) and N_4O_5 (Dy2 and Dy3) coordination environments respectively. Adjacent Dy^{3+} ions are connected by two μ_2 -O bridges from hydrazone oxygen of two ligands with bridging angles in the range of $114.5(2)$ - $117.9(2)^\circ$. Distances between neighboring Dy^{3+} ions are $4.103(5)$ Å and $4.105(5)$ Å. Dy- O bond distances are lying in the range of $2.339(4)$ Å to $2.472(4)$ Å and Dy-N bond distances are lying in the range of $2.452(5)$ Å to $2.640(6)$ Å. Because of the different crystal system with compare to **1**, packing diagram of complex **2** is different and it forms double helical arrangement along the crystallographic *a* axis through intra-molecular (Fig. S9) intermolecular (Fig. S10) hydrogen bonding (Table S2) (Fig. 4, right). The complex also involved two intermolecular π - π interactions through pyridine rings (centroid-centroid distance = 3.925 Å, shift distance = 1.899 Å and centroid-centroid distance = 3.579 Å, shift distance = 1.426 Å) (Fig. S11).

Table 1. Summary of crystallographic data for complexes **1-4**

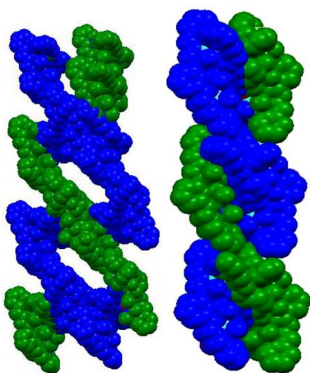
Molecule	1	2	3	4
Formula	$C_{38}H_{62}Gd_3O_{22}N_{14}Cl_5$	$C_{38}H_{56}Dy_3O_{19}N_{14}Cl_5$	$C_{64}H_{88}Cl_2Gd_6N_{16}O_{32}$	$C_{64}H_{88}Cl_2Dy_6N_{16}O_{32}$
Mr	1716.00	1677.70	2607.87	2639.37
Crystal System	Monoclinic	Triclinic	Monoclinic	Monoclinic
Space Group	<i>C2/c</i>	<i>P-1</i>	<i>P21/c</i>	<i>P21/c</i>
<i>a</i> / Å	19.6915(13)	9.6026(10)	13.942(4)	13.8677(16)
<i>b</i> / Å	16.9653(12)	17.0196(17)	16.159(4)	16.1876(19)
<i>c</i> / Å	20.2970(14)	18.5657(18)	20.385(6)	20.268(2)
α / °	90.00	93.555(5)	90.00	90.00

$\beta/^\circ$	96.649(4)	94.076(5)	103.577(14)	103.230(5)
$\gamma/^\circ$	90.00	98.263(5)	90.00	90.00
V/Å	6735.1(8)	2987.1(5)	4464(2)	4429.1(9)
Z	4	2	2	2
Dc/g cm ⁻³	1.692	1.857	1.940	1.976
μ (Mo-K α)/cm-1	0.71073	0.71073	0.71073	0.71073
Reflection	5880	13650	8303	7772
Unique Refelctions	5221	13400	6024	6699
R ₁ ^a	0.0426	0.0473	0.0528	0.0415
wR ₂ ^b	0.1175	0.1409	0.1616	0.1224

$$^aR_1 = \frac{\sum ||F_o| - |F_c||}{\sum |F_o|}, \quad ^b wR_2 = \left[\frac{\sum w(F_o^2 - F_c^2)^2}{\sum (F_o^2)^2} \right]^{1/2}$$



5 **Fig. 3.** Ball & stick model showing molecular structure of complex **2** in the crystal. Colour code: yellow, dysprosium; red, oxygen; blue, nitrogen; gray, carbon; Hydrogen atoms and solvents are omitted for clarity.



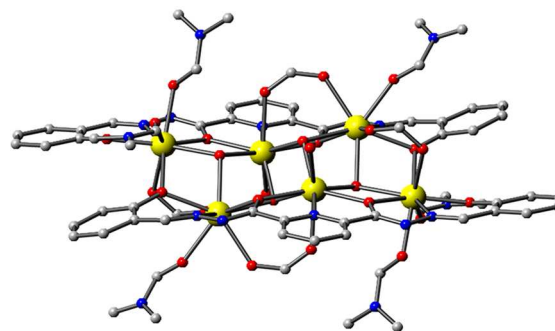
10 **Fig. 4.** Spacefilling representation of the double zig-zag like architecture of complex **1** (left) and **2** (right) along *a*-axis.

Structural Description for **3** and **4**

The complexes **3** and **4** crystallise in *P2₁/c* space group. These complexes are isostructural hexanuclear cages comprising of six Ln³⁺ ions (Ln=Gd, Dy), two [L²]⁴⁺ ligands, four formate ligands, four μ_3 -OH and six coordinated DMF molecules (Fig. 5). In addition to this four non-coordinated water molecules and two Cl⁻ anions are also present in the crystal lattice which balances the overall charge of the complexes.

20 All the metal centers in both complexes **3** and **4** are octa-coordinated (N₁O₇) and show square antiprismatic geometry (Fig. S12). The formate ligands show a $\mu_{1,1}$ coordination mode. In

complex **3**, the Gd-O and Gd-N bond lengths are in the range of 2.220(7)-2.458(7) Å and 2.514(9)-2.575(8) Å respectively. Dy-O and Dy-N bond distances in complex **4** range between 2.180(6)-2.427(7) Å and 2.500(8)-2.543(8) Å respectively. All the Ln- μ_3 -OH bond distances fall in the normal range of 2.317-2.454 Å.¹⁶ Distances between two adjacent metal centers for both the complexes fall in between 3.706(7) Å-3.910(1) Å and the Ln-O-Ln bond angles are in the range of 102.1(2)-111.6(2)^o. The core structure shows that the μ_3 -hydroxo metal triangles generate four distorted hemi-cubane like units. Each hemi-cubane unit shares both edges and vertices with its neighbouring units to form overall structure (Fig. 6). The ligand environment of terminal hemi-cubanes include two μ_2 -O groups from the ligand and two μ_3 -hydroxo groups while for central ones it is one μ_2 -O group of the ligand and three μ_3 -hydroxo groups. For both the terminal and central hemi-cubanes, μ_3 -hydroxo groups do not bridge symmetrically to the three metal centers (2.317 Å-2.454(5) Å). Similar is the case with the μ_2 -O groups of the terminal hemi-cubanes (2.331(5) Å-2.458(7) Å). However, μ_2 -O groups that connect the terminal hemicubanes with the central ones bridge symmetrically (2.349(6) Å). Packing diagram of both the complexes **3** and **4** show zig-zag like arrangement along *c*-axis (Fig. S13).



50 **Fig. 5.** Ball & stick model showing molecular structure of **4** in the crystal. Colour code: same as in **1**; Colour code: yellow, dysprosium; red, oxygen; blue, nitrogen; gray, carbon; Hydrogen atoms are omitted for clarity.

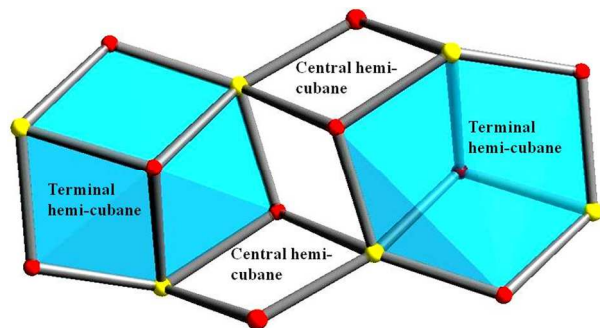


Fig. 6. Core structure of complex **4**. Colour code: same as in Fig. 5; Hydrogen and carbon atoms are omitted for clarity.

Magnetic Study

For magnetic characterization dc susceptibility data of complexes **1-4** were collected on polycrystalline samples in the temperature range of 1.8-300 K at 0.1 T and are shown in the form of $\chi_M T$ (χ_M = molar magnetic susceptibility) vs. temperature (T) plot in Fig. 7 and 13.

Complexes **1** and **3**:

Magnetic properties of complexes **1** and **3** are discussed together as both of them contain Gd^{3+} as metal ion. The observed room temperature $\chi_M T$ values for **1** and **3** are $24.3 \text{ cm}^3 \text{ mol}^{-1} \text{ K}$ and $46.5 \text{ cm}^3 \text{ mol}^{-1} \text{ K}$ respectively and the values are close to the spin only value ($23.4 \text{ cm}^3 \text{ mol}^{-1} \text{ K}$ for three uncoupled Gd^{3+} and $46.8 \text{ cm}^3 \text{ mol}^{-1} \text{ K}$ for six uncoupled Gd^{3+} for $g = 2$) (Fig. 7). For both **1** and **3**, $\chi_M T$ values are almost constant up to ~ 20 K, below which it increases to reach the value of $26.57 \text{ cm}^3 \text{ mol}^{-1} \text{ K}$ for **1** and decreases down to the value of $20.94 \text{ cm}^3 \text{ mol}^{-1} \text{ K}$ for **3** at 1.8 K.

This may be due to weak ferromagnetic and antiferromagnetic interactions present at low temperature respectively. As the Gd^{3+} ions show no spin orbit coupling of the first order, therefore attempt has been made to estimate magnetic interactions for both the complexes. For **1**, experimental $\chi_M T$ vs. T plot was fitted using the Hamiltonian (1) based on the model given in Fig. 8. The best fit afforded $g = 2.02$, $J1 = 0.025 \text{ cm}^{-1}$ and $J2 = 0.003 \text{ cm}^{-1}$ which suggest presence of weak ferromagnetic interactions among the metals centers in **1**. Where $J1$ corresponds to interaction between adjacent metal centers through $\mu_2\text{-O}$ and $J2$ corresponds to interaction between nearest neighbours through conjugated ligands. Although both the interactions are weak, however, interaction via $J2$ is even weaker due to larger separation between the metal centers. For **3**, experimental $\chi_M T$ vs. T plot was fitted using the Hamiltonian (2) based on the model given in Fig. 9. The data was fitted nicely with the $g = 2.0$, $J1 = -0.10 \text{ cm}^{-1}$ and $J2 = -0.02 \text{ cm}^{-1}$ suggesting weak antiferromagnetic interactions between the Gd^{3+} centres. Similar to **1**, we can suggest that the weaker interaction via $J2$ is due to large separation between the metal centres.

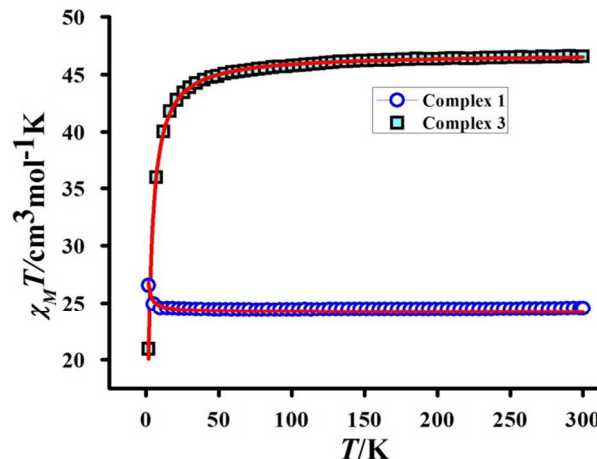


Fig. 7. Temperature dependence of $\chi_M T$ plot for **1** and **3** measured at an applied field of 0.1 T and red lines are the best fit obtained.

Magnetization measurements at low temperature (Fig. 10) show saturation values of $20.6 \text{ N}\mu_B$ and $41.7 \text{ N}\mu_B$ at 7 T for complexes **1** and **3** respectively. These are in well agreement with the theoretical values of $21 \text{ N}\mu_B$ and $42 \text{ N}\mu_B$ for three and six isolated Gd^{3+} respectively ($g = 2$).

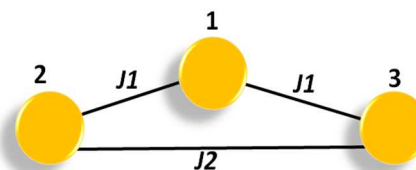


Fig. 8. Model used for the data fitting of complex **1**. Balls represent metal centers and lines represent connectivity between two metal centers.

$$H_{Gd_3} = -J1(S_1S_2 + S_1S_3) - J2S_2S_3 - g\mu_B H \cdot \sum_{i=1}^3 S_i \dots (1)$$

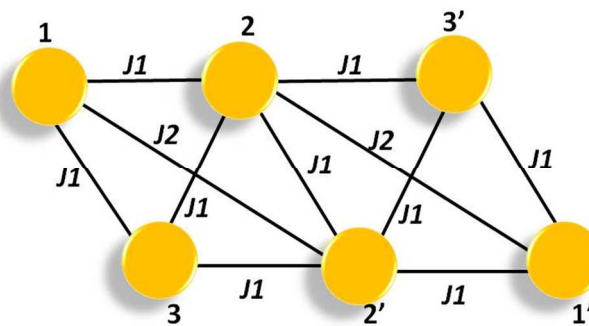


Fig. 9. Model used for the data fitting of complex **3**. Balls represent metal centers and lines represent connectivity between two metal centers.

$$H_{Gd_6} = -J1(S_1S_2 + S_1S_3 + S_2S_3 + S_2S_3' + S_2S_2' + S_2S_3' + S_2S_1' + S_1S_3') - J2(S_1S_2' + S_2S_1') - g\mu_B H \cdot \sum_{i=1}^6 S_i \dots (2)$$

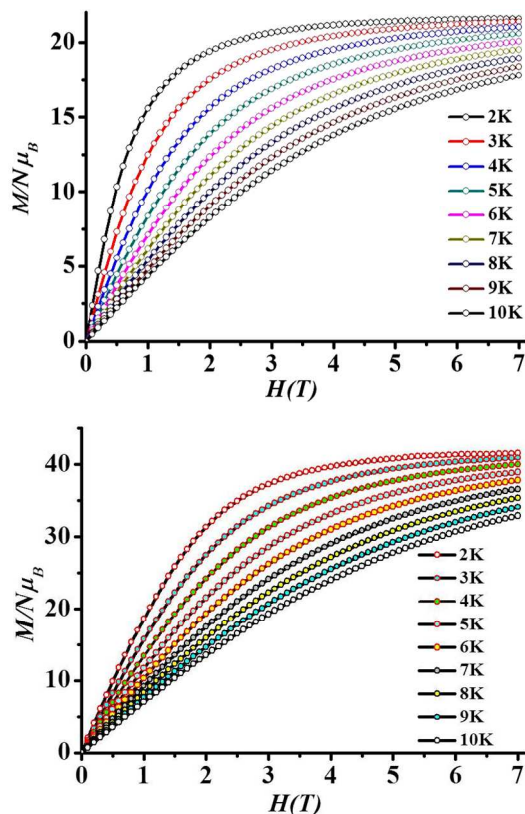


Fig. 10. Field-dependencies of isothermal normalized magnetizations for complex 1 (top) and complex 3 (bottom), collected for temperatures ranging from 2 to 10 K. Red lines are the best fit obtained.

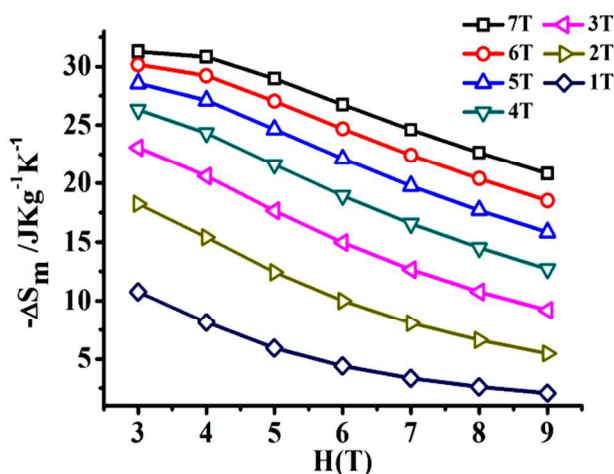


Fig. 11. Temperature dependencies (3 to 10 K) of magnetic entropy change ($-\Delta S_m$) for complex 1 as obtained from the magnetization data.

The magnetic entropy changes (ΔS_m) and hence the MCE for 1 and 3 were calculated using the Maxwell equation $\Delta S_m(T)_{\Delta H} = \int [\partial M(T, H) / \partial T]_H dH$. The resulting ΔS_m values for both the complexes are gradually increased with lowering the temperature from 9 K to 2 K (Fig. 11-12). The highest value of $31.3 \text{ Jkg}^{-1}\text{K}^{-1}$ and $33.5 \text{ Jkg}^{-1}\text{K}^{-1}$ were obtained at 2 K and 7 T for 1 and 3 respectively. Corresponding volumetric entropy changes are $53.4 \text{ mJcm}^{-3}\text{K}^{-1}$ and $63.7 \text{ mJcm}^{-3}\text{K}^{-1}$ for 1 and 3 respectively. These values are quite significant for any discrete cage system. Higher

$[\Delta S_m]$ value of complex 3 than 1 can be explained by considering 20 mol. wt./no. of metal ratio (For 1, 572.3 and for 3, 426.98) which is key parameter to determine the MCE.

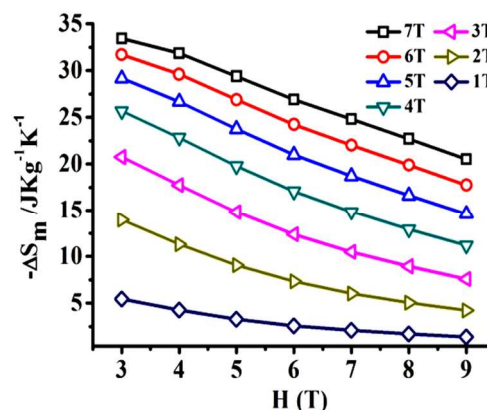


Fig. 12. Temperature dependencies (3 to 10 K) of magnetic entropy change ($-\Delta S_m$) for complex 3 as obtained from magnetization data.

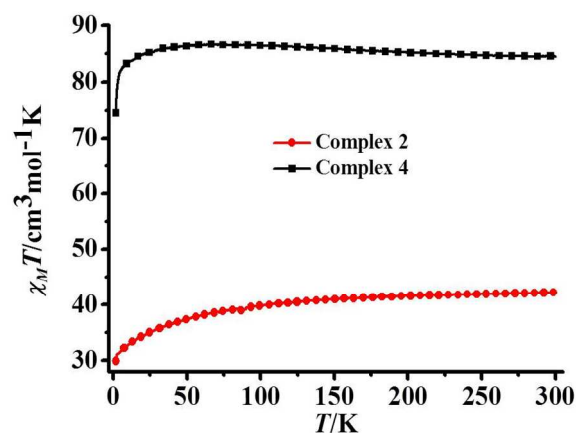


Fig. 13. Temperature dependence of $\chi_M T$ plot for complex 2 and 4 measured at 0.1 T.

Complexes 2 and 4:

Magnetic properties of complexes 2 and 4 are discussed together as both of them contain Dy^{3+} as metal ion. The room temperature $\chi_M T$ values are $42.2 \text{ cm}^3\text{mol}^{-1}\text{K}$ and $84.5 \text{ cm}^3\text{mol}^{-1}\text{K}$ for 2 and 4 respectively which are close to the calculated spin-orbit values $42.5 \text{ cm}^3\text{mol}^{-1}\text{K}$ and $85.0 \text{ cm}^3\text{mol}^{-1}\text{K}$ for three and six isolated Dy^{3+} (${}^6\text{H}_{15/2}$, $S = 5/2$, $L = 5$, $g = 4/3$) (Fig. 13). For 2, the $\chi_M T$ value decreases gradually from room temperature with decreasing temperature and reached to a value of $35.6 \text{ cm}^3\text{mol}^{-1}\text{K}$ at 30 K. Whereas for 4, it is almost constant up to ~ 20 K. For both the molecules $\chi_M T$ values decrease with temperature and finally drop to $29.9 \text{ cm}^3\text{mol}^{-1}\text{K}$ for 2 and $74.5 \text{ cm}^3\text{mol}^{-1}\text{K}$ for 4 at 1.8 K implying presence of antiferromagnetic interaction in the molecule and that is largely because of the thermal depopulation of excited Stark sublevels (16-fold degeneracy of the ${}^6\text{H}_{15/2}$ ground state). Because of the spin-orbit coupling it is not possible to fit the experimental $\chi_M T$ vs T plot for complexes 2 and 4. $M/N\mu_B$ vs H plots for 2 and 4 do not show any saturation even at the field of 7 T, suggesting the presence of magnetic anisotropy and significant crystal-field effects from the Dy(III) ions (Fig. 14-15).

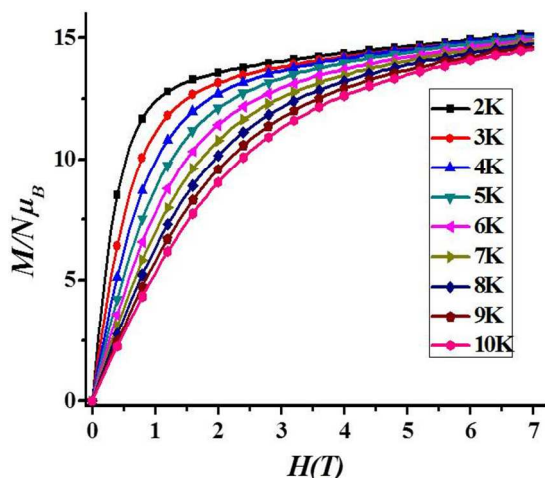


Fig. 14. Field-dependencies of isothermal normalized magnetizations for complex 2 collected for temperatures ranging from 2 to 10 K

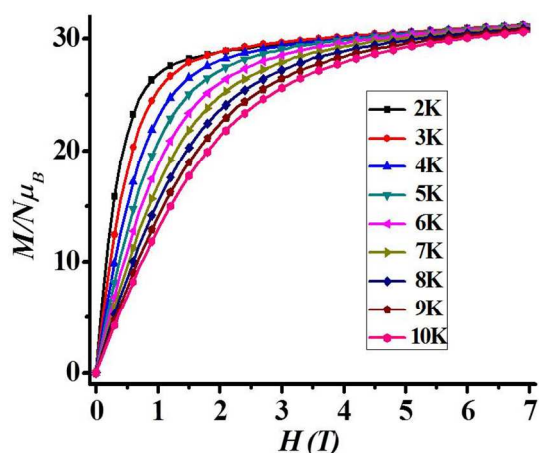


Fig. 15. Field-dependencies of isothermal normalized magnetizations for complex 4 collected for temperatures ranging from 2 to 10 K.

Moreover non-superposition of M vs H/T plot (Fig. S14-S15) confirms the presence of magnetic anisotropy present in the molecule. Experimental magnetization values reach up to $15.2 N\mu_B$ and $31.2 N\mu_B$ for **2** and **4** respectively at 2 K and 7 T which are close to the theoretical values of $15.7 N\mu_B$ and $31.4 N\mu_B$ for corresponding three and six non interacting Dy^{3+} ions in a crystal field environment.

AC measurements for **2** and **4** were performed at 1.8-10 K in the frequency range of 1-780 Hz at zero dc fields to examine the SMM behavior. In phase components of ac susceptibility (χ') are frequency independent for complex **2** and frequency dependent for complex **4** (Fig. 16-17). But both the complexes **2** and **4** show frequency dependency of out of phase component (χ'') of ac susceptibilities which indicates slow relaxation of magnetization with characteristic SMM behavior (Fig. 18), 20 (top)). The graphical representation of χ'' vs χ' process for complex **2** and **4** (Fig. S16) (Cole-Cole plot)¹⁷ in the temperature range of 2-7.1 K showing the evidence for slow relaxation.

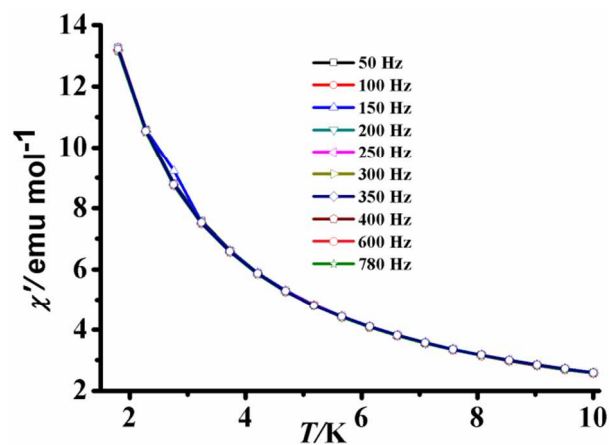


Fig. 16. Frequency dependence of the in phase (χ') ac susceptibility for complex 2 under a zero dc field.

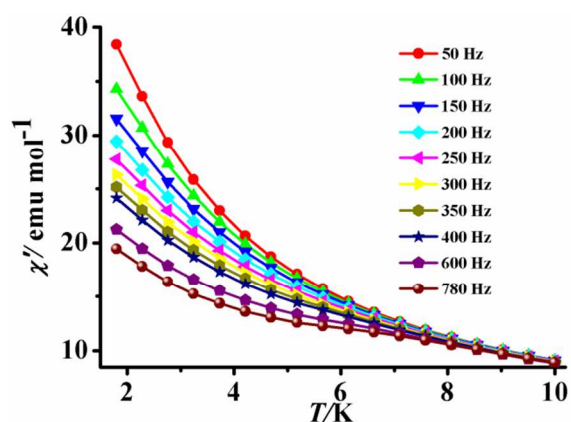


Fig. 17. Frequency dependence of the in phase (χ') ac susceptibility for complex 4 under a zero dc field.

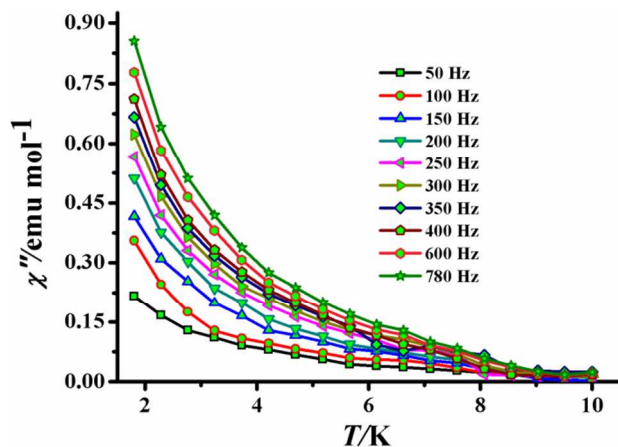


Fig. 18. Frequency dependence of the out of phase (χ'') ac susceptibility for complex 2 under a zero dc field.

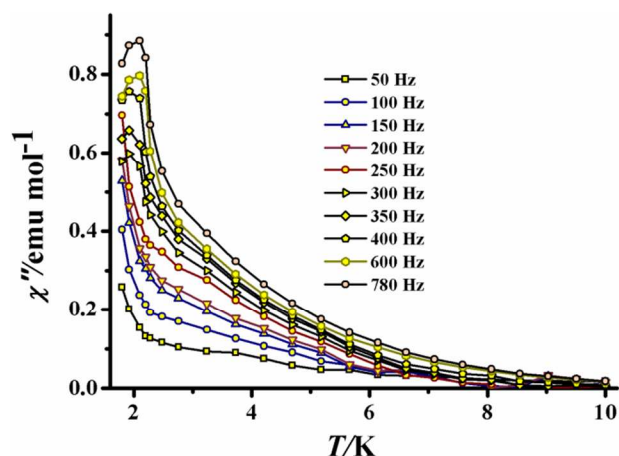


Fig. 19. Frequency dependence of the out of phase (χ'') ac susceptibility for complex 2 under a field of 1400 Oe.

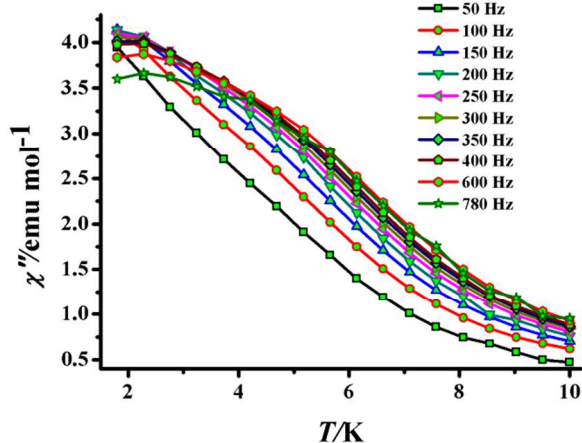
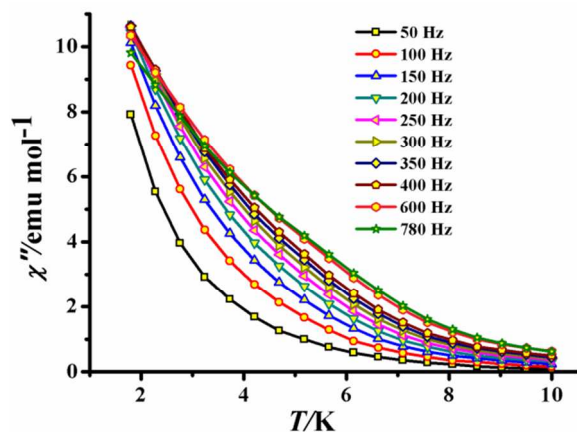


Fig. 20. Frequency dependence of the out of phase (χ'') ac susceptibility for complex 4 under a zero dc field (top) and under a field of 1800 Oe (bottom).

Nearly symmetrical distribution of Cole-Cole plot for 4 indicates the single relaxation process. Due to quantum tunneling of magnetization (QTM) phenomenon¹⁸⁻¹⁹ clear full maxima were not observed both in χ'' and χ' of the ac susceptibilities for both 2 and 4. In order to reduce QTM, ac measurements in the presence of different static dc field were performed (Figs. S17-S18). At optimized dc field of 1400 Oe, frequency dependency of χ' vs. T

plot (Fig. S19, left) and few maxima of χ'' vs. T (Fig.19) were observed for complex 2. For complex 4, at optimized dc field of 1800 Oe, frequency dependency of χ' vs. T plot (Fig. S19, right) was observed and χ'' vs. T show the appearance of broad maxima (Fig. 20, bottom) that further suggests the process of the slow magnetic relaxation. In order to determine the effective anisotropy energy barrier (U_{eff}) and relaxation time (τ_0), $\ln(\chi''/\chi')$ vs $1/T$ plots were deduced from the χ'' vs. T and χ' vs. T data and the plots were fitted with the Debye equation:

$$\ln(\chi''/\chi') = \ln(\omega\tau_0) + U_{\text{eff}}/kT \dots\dots(1)$$

where, k is the Boltzmann constant and $1/\tau_0$ is the pre-exponential factor (Figs. 21-22). From the fitting of the plots $U_{\text{eff}} = 11.2$ K and $\tau_0 = 3.1 \times 10^{-6} \text{ sec}^{-1}$ for complex 2 and $U_{\text{eff}} = 9.7$ K and $\tau_0 = 6.4 \times 10^{-6} \text{ sec}^{-1}$ for complex 4 were obtained.

The nature and symmetry of the coordination geometry and crystal field determine the magnetic anisotropy and can influence anisotropy energy barrier. All the Dy^{3+} centers comprise of tri-capped trigonal prismatic geometry in complex 2 and square antiprismatic geometry in complex 4. This disparity in geometry effects the orientation of the easy-axes and magneto anisotropy which result the difference in anisotropy energy barrier.

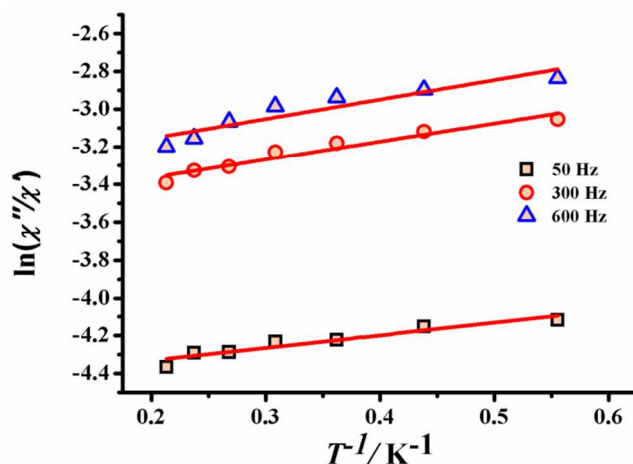


Fig. 21. Natural logarithm of the ratio of χ'' over χ' vs. $1/T$ for complex 2. Red lines represent best fit obtained from equation (1).

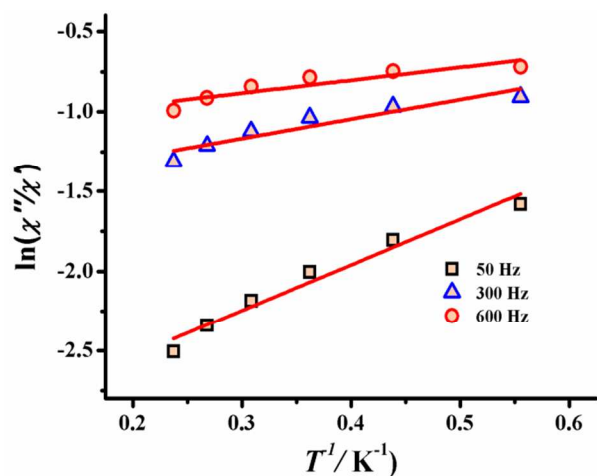


Fig. 22. Natural logarithm of the ratio of χ'' over χ' vs. $1/T$ for complex 4. Red lines represent best fit obtained from equation (1).

CONCLUSION

In summary, we have prepared two multidentate ligands and they were reacted to obtain a family of multinuclear lanthanide complexes. Slight change in coordination cavity of the ligands resulted vivid change in nuclearity of the complexes. Structural and magnetic characterizations were done for all complexes. The Dy complexes are characterized as SMMs with energy barrier (U_{eff}) of 11.2 K and relaxation time (τ_0) $3.1 \times 10^{-6} \text{ sec}^{-1}$ for **2** and $U_{\text{eff}} = 9.7 \text{ K}$ and $\tau_0 = 6.4 \times 10^{-6} \text{ sec}^{-1}$ for complex **4**. The entropy changes (ΔS_m) and hence the MCE for Gd complexes (**1** and **3**) were calculated, which gives the moderate value of $31.3 \text{ J kg}^{-1}\text{K}^{-1}$ and $33.5 \text{ J kg}^{-1}\text{K}^{-1}$ at 3 K and 7 T for **1** and **3** respectively.

AA and JAS acknowledge CSIR for their SRF fellowships. SB thanks IISER Bhopal for the PhD fellowship. SK thanks DST, Government of India (Project No. SR/FT/CS-016/2010) and IISER Bhopal for generous financial and infrastructural support.

Notes and references

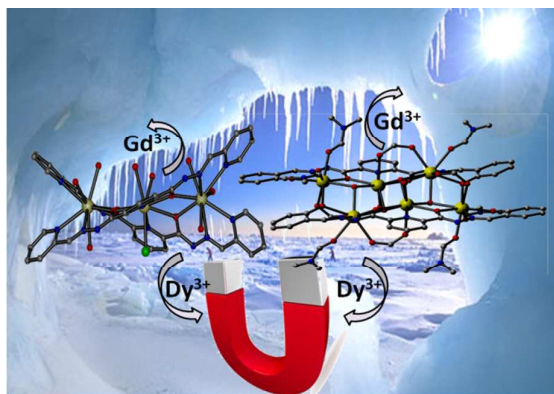
Department of Chemistry, IISER Bhopal, Bhopal 462066, MP, INDIA, Fax: +91-755-6692392; Tel: +91-755-6692339

E-mail: skonar@iiserb.ac.in

Dedicated to Prof. Ashutosh Ghosh on the occasion of his 55th Birthday

† Electronic Supplementary Information (ESI) available: Additional synthetic and magnetic data for all compounds. See DOI: 10.1039/b000000x/

- (1) (a) D. Gatteschi, R. Sessoli and J. Villain, *Molecular Nanomagnets*, Oxford University Press, New York, 2006; (b) F. S. Guo, J. L. Liu, J. D. Leng, Z. S. Meng, Z. J. Lin, M. L. Tong, S. Gao, L. Ungur and L. F. Chibotaru, *Chem. Eur. J.*, 2011, **17**, 2458; (c) D. Gatteschi, A. Caneschi, L. Pardi and R. Sessoli, *Science*, 1994, **265**, 1054; (d) R. Sessoli, H. L. Tsai, A. R. Schake, S. Wang, J. B. Vincent, K. Folting, D. Gatteschi, G. Christou and D. N. Hendrickson, *J. Am. Chem. Soc.*, 1993, **115**, 1804.
- (2) (a) R. Sibille, T. Mazet, B. Malaman and M. François, *Chem. Eur. J.*, 2012, **41**, 12970; (b) G. Lorusso, M. A. Palacios, G. S. Nichol, E. K. Brechin, O. Roubeau and M. Evangelisti, *Chem. Commun.* 2012, **48**, 7592; (c) Y. N. Guo, X. H. Chen, S. Xue and J. Tang, *Inorg. Chem.*, 2011, **50**, 9705.
- (3) (a) M. Evangelisti, F. Luis, L. J. Jongh and M. J. Affronte, *Mater. Chem.* 2006, **16**, 2534; (b) M. Evangelisti and E. K. Brechin, *Dalton Trans.* 2010, **39**, 4672.
- (4) (a) R. Sessoli, *Angew. Chem. Int. Ed.* 2012, **51**, 43; (b) G. Karotsis, M. Evangelisti, S. J. Dalgarno and E. K. Brechin, *Angew. Chem., Int. Ed.* 2009, **48**, 9928; (c) G. Karotsis, S. Kennedy, S. J. Teat, C. M. Beavers, D. A. Fowler, J. J. Morales, M. Evangelisti, S. J. Dalgarno and E. K. Brechin, *J. Am. Chem. Soc.* 2010, **132**, 12983; (d) J. B. Peng, Q. C. Zhang, X. J. Kong, Y. P. Ren, L. S. Long, R. B. Huang, L. S. Zheng, Z. P. Zheng, *Angew. Chem. Int. Ed.* 2011, **50**, 10649; (e) M. Evangelisti, O. Roubeau, E. Palacios, A. Camon, T. N. Hooper, E. K. Brechin and J. J. Alonso, *Angew. Chem. Int. Ed.* 2011, **50**, 6606; (f) J. W. Sharples, Y. Z. Zheng, F. Tuna, E. J. McInnes and D. Collison, *Chem. Commun.* 2011, **47**, 7650; (g) Y. Z. Zheng, M. Evangelisti and R. E. P. Winpenny, *Chem. Sci.* 2011, **2**, 99; (h) S. K. Langle, N. F. Chilton, B. Moubaraki, T. Hooper, E. K. Brechin, M. Evangelisti and K. S. Murray, *Chem. Sci.* 2011, **2**, 1166; (i) Y. Z. Zheng, M. Evangelisti and R. E. P. Winpenny, *Angew. Chem. Int. Ed.* 2011, **50**, 3692; (j) A. Hosoi, Y. Yukawa, S. Igarashi, S. J. Teat, O. Roubeau, M. Evangelisti, E. Cremades, E. Ruiz, L. A. Barrios and G. Aromi, *Chem. Eur. J.* 2011, **17**, 8264; (k) Y. Z. Zheng, M. Evangelisti, F. Tuna and R. E. P. Winpenny, *J. Am. Chem. Soc.* 2012, **134**, 1057; (l) T. Birk, K. S. Pedersen, C. A. Thuesen, T. Weyhermüller, M. Schau-Magnussen, S. Piligkos, H. Weihe, S. Mossin, M. Evangelisti and J. Bendix, *Inorg. Chem.* 2012, **51**, 5435; (m) A. Adhikary, J. A. Sheikh, A. D. Konar and S. Konar, *RSC Adv.* 2014, **4**, 12408.
- (5) F. S. Guo, J. D. Leng, J. L. Liu, Z. S. Meng and M. L. Tong, *Inorg. Chem.* 2012, **51**, 405.
- (6) L. Sedláčková, J. Hanko, A. Orendáčová, M. Orendáč, C. L.; Zhou, W. H.; Zhu, B. W. Wang, Z. M. Wang and Gao, S. *J. Alloys Compd.* 2009, **487**, 425.
- (7) M. J. Martínez-Peñáz, O. Montero, M. Evangelisti, F. Luis, J. Sese, S. Cardona-Serra and E. Coronado, *Adv. Mater.* 2012, DOI: 10.1002/adma.201200750.
- (8) (a) J. W. Sharples, Y. Z. Zheng, F. Tuna, E. J. L. McInnes and D. Collison, *Chem. Commun.* 2011, **47**, 7650; (b) R. Shaw, R. H. Laye, L. F. Jones, D. M. Low, C. T. Eeckelaers, Q. Wei, C. J. Milios, S. Teat, M. Helliwell, J. Raftery, M. Evangelisti, M. Affronte, D. Collison, E. K. Brechin, and E. J. L. McInnes, *Inorg. Chem.* 2007, **46**, 4968; (c) M. Evangelisti, A. Candini, A. Ghirri, M. Affronte, E. K. Brechin and E. J. L. McInnes, *Appl. Phys. Lett.*, 2005, **87**, 072504; (d) Z. G. Wang, J. Lu, C. Y. Gao, C. Wang, J. L. Tian, W. Gu, X. Liu and S. P. Yan, *Inorg. Chem. Commun.* 2013, **27**, 127. (e) N. Ishikawa, M. Sugita, T. Ishikawa, S. Y. Koshihara, and Y. J. Kaizu, *J. Phys. Chem. B*, 2004, **108**, 11265.
- (9) (a) G. Aromi and E. K. Brechin, *Struct. Bond*, 2006, **122**, 1; (b) M. Evangelisti and E. K. Brechin, *Dalton Trans.*, 2010, **39**, 4672; (c) G. Karotsis, M. Evangelisti, S. J. Dalgarno and E. K. Brechin, *Angew. Chem. Int. Ed.* 2009, **48**, 9928; (d) Y. Z. Zheng, M. Evangelisti, and R. E. P. Winpenny, *Chem. Sci.* 2011, **2**, 99.
- (10) (a) R. Sessoli and A. K. Powell, *Coord. Chem. Rev.*, 2009, **253**, 2328; (b) J. D. Reinhart, M. Fang, W. J. Evans and J. R. Long, *Nat. Chem.* 2011, **3**, 538.
- (11) (a) A. Adhikary, S. Goswami, J. A. Sheikh and S. Konar, *Eur. J. Inorg. Chem.*, 2014, 963; (b) A. Adhikary, H. S. Jena, S. Khatua and S. Konar, *Chem. Asian J.*, DOI: 10.1002/asia.201301619; (c) M. U. Anwar, S. S. Tandon, L. N. Dawe, F. Habib, M. Murugesu and L. K. Thompson, *Inorg. Chem.* 2012, **51**, 1028.
- (12) G. Sheldrick, *SHELXL-97, Program for Crystal Structure Refinement*; University of Gottingen: Gottingen, Germany, 1997.
- (13) (a) A. L. Spek, *J. Appl. Crystallogr.* 2003, **36**, 7. (b) L. J. Farrugia, *J. Appl. Crystallogr.* 1999, **32**, 837.
- (14) O. Kahn, *Molecular Magnetism*, VCH: New York, 1993.
- (15) (a) A. Bacchi, M. Carcelli, P. Pelagatti, C. Pelizzi, G. Pelizzi and F. Zani, *J. Inorg. Biochem.* 1999, **75**, 123. (b) X. Chen, S. Zhan, C. Hu, Q. Meng and Y. Liu, *J. Chem. Soc., Dalton Trans.* 1997, 245.
- (16) (a) O. A. Gerasko, E. A. Mainicheva, M. I. Naumova, M. Neumaier, M. M. Kappes, S. Lebedkin, D. Fenske and V. P. Fedin, *Inorg. Chem.* 2008, **47**, 8869; (b) P.-F. Shi, Y.-Z. Zheng, X.-Q. Zhao, G. Xiong, B. Zhao, F.-F. Wan and P. Cheng, *Chem. Eur. J.* 2012, **18**, 15086; (c) Y.-L. Hou, G. Xiong, P.-F. Shi, R.-R. Cheng, J.-Z. Cui and B. Zhao, *Chem. Commun.* 2013, **49**, 6066; (d) C.-H. Zeng, F.-L. Zhao, Y.-Y. Yang, M.-Y. Xie, X.-M. Ding, D.-J. Houa, S. Weng, *Dalton Trans.* 2013, **42**, 2052.
- (17) (a) K. S. Cole and R. H. Cole, *J. Chem. Soc.* 1941, **9**, 341; (b) S. M. J. Aubin, Z. Sun, L. Pardi, J. Krzystek, K. Folting, L. J. Brunel, A. L. Rheingold, G. Christou and D. N. Hendrickson, *Inorg. Chem.* 1999, **38**, 5329.
- (18) M. Jeletic, P.-H. Lin, J. Le Roy, I. Korobkov, S. I. Gorelsky and M. Murugesu, *J. Am. Chem. Soc.* 2011, **133**, 19286.
- (19) F. Habib, P.-H. Lin, J. Long, I. Korobkov, W. Wernsdorfer and M. Murugesu, *J. Am. Chem. Soc.* 2011, **133**, 8830.



Hydrazone based four lanthanide complexes were synthesized where two gadolinium complexes show significant magnetocaloric effect and its dysprosium analogue show SMM behaviors.